Argyrotoxins A-C, a trisubstituted dihydroisobenzofuranone, a tetrasubstituted 2-hydroxyethylbenzamide and a tetrasubstitutedphenyl trisubstitutedbutyl ether produced by Alternaria argyroxiphii, the causal agent of leaf spot on African mahogany trees (Khaya senegalensis)

(Article begins on next page)

23 December 2024

Argyrotoxins A-C, a trisubstituted dihydroisobenzofuranone, a tetrasubstituted 2-hydroxyethylbenzamide and a tetrasubstitutedphenyl trisubstitutedbutyl ether produced by Alternaria argyroxiphii, the causal agent of leaf spot on African mahogany trees (Khaya senegalensis)

Marco Masi[a], Roberta Di Lecce[a], Lucia Maddau[b], Giulia Marsico[c], Stefano Superchi[c], Antonio Evidente[a,*]

[a] Dipartimento di Scienze Chimiche, Università di Napoli Federico II, Complesso Universitario Monte Sant'Angelo, Via Cintia 4, 80126, Napoli, Italy

[b] Dipartimento di Agraria, Sezione di Patologia Vegetale ed Entomologia, Università degli Studi di Sassari, Viale Italia 39, 07100, Sassari, Italy

[c] Dipartimento di Scienze, Università della Basilicata, Viale dell'Ateneo Lucano 10, 85100, Potenza, Italy

ABSTRACT: Three previously undescribed metabolites named argyrotoxins A-C, were isolated, together with the well known porritoxinol, its closely related phthalide, a phthalide derivative, zinniol, alternariol and its 4-methyl ether from *Alternaria argyroxiphii* E.G. Simmons & Aragaki, the causal agent of leaf spot on African mahogany trees, *Khaya senegalensis* A. Juss. (Meliaceae). The known compounds were identified comparing their physical and spectroscopic properties to those previously reported in literature. Argyrotoxins A-C were characterized essentially by NMR (^{1}H, ^{13}C, COSY, HSQC, HMBC and NOESY NMR spectra) and HRESIMS spectra as 4-(7-methoxy-6-methyl-3-oxo-1,3-dihydro-isobenzofuran-5-yloxy)-2-methyl-butyric acid, 5-but-2-enyloxy-N-(2-hydroxyethyl)-2-hydroxymethyl-3-methoxy-4-methyl-benzamide and 1-(5-(hydroxymethyl)-3-methoxy-4-(methoxymethyl)-2-methylphenoxy)-3-methylbutane-2,3-diol, respectively. The absolute configuration of argyrotoxin A was determined through electronic circular dichroism, by applying the biphenyl chiroptical probe approach. The phytoxicity of all metabolites isolated was evaluated by leaf puncture assay at concentration of 1 mg/mL. Zinniol proved to be the most active compound causing necrotic lesions on young leaves of *Hedera elix* L., *Phaseolus vulgaris* L. and *Quercus ilex* L. Argirotoxins A and B were found active, to a minor extent, on *Phaseolus vulgaris* L. leaves, while porritoxinol exhibited activity on holm oak leaves. The other secondary metabolites herein reported for *A. argyroxiphii* were inactive.

1. Introduction

Mahogany wood is obtained from different species of the genus *Swietenia* and *Khaya* and possesses important technological characteristics that determine its high commercial value (Falesi and Baena, 1999; Pinheiro et al., 2001). *Khaya senegalensis* A. Juss. (Meliaceae), known as African mahogany, is one of the plant included in the genus *Khaya*. It is native of tropical Africa and Madagascar but it was planted in Brazil since 1976 (Falesi and Baena, 1999) as a consequence of the strong decrease of the native Brazilian mahogany *Swietenia macrophylla* King in Hook (Pinheiro et al., 2001) due to devastating losses induced by *Hypsipyla grandella* Zellar (the pest insect known as the mahogany shoot borer). This problem prompted the prohibition of exportation and marketing of native Brazilian mahogany wood and since 2000 the commercial use of African mahogany was suggested (Gasparotto et al., 2001; Couto et al., 2004).

However, even African mahogany imported in Brazil was soon found affected by different pathogens. Among them, *Alternaria argyroxiphii* E.G. Simmons & Aragaki (Simmons 2007; Woudenberg et al., 2013) was reported as the cause of leaf spot on African mahogany trees since 2017, even if the disease was already previously observed in Minas Gerais State, Brazil, on October 2012. A pathogenicity test, carried out to fulfil Koch's postulates, confirmed *A. argyroxiphii* as a causal agent of leaf spot of *K. senegalensis* (Teixeira et al., 2017). *Alternaria* is a well known phytotoxin producer fungal genus (Strobel, 1982; Cimmino et al., 2015; Pontes et al., 2020) as well as other genera that infect forest plants (Masi et al., 2018b). Phytotoxins produced by *Alternaria* species and belonging to different compounds families were reported to show important virulence features (Strobel, 1982; Cimmino et al., 2015; Pontes et al., 2020). Several examples of *Alternaria* phytotoxins, involved in plant disease causing heavy economical losses, are reported, such as the phytotoxin zinniol (**7**, Fig. 1). Phytotoxin **7** was produced by different species including *Alternaria zinniae* H. Pape ex M.B. Ellis, the causal agent of

common leaf spot and seedling blight of zinnia, sunflower and marigolds (White and Starrat, 1967) and by *Alternaria solani* Sorauer, Z. PflKrankh (Stoessl et al., 1979), the causal agent of tomato and potato early blight. The latter fungus also produced altersolanols A and B, belonging to a small group of tetrahydroanthraquinones, with interesting antibiotic activity (Becker et al., 1978). These metabolites were also isolated from the mycelium of *Alternaria porri* (Ellis) Cif., the causal agent of black spot disease in the stone-leek and onion, together with porritoxinol (**4**, Fig. 1), a zinniol-like metabolite, tentoxin, porritoxin and silvaticol (Suemitsu et al., 1978). *Alternaria sonchi* J.J. Davis, proposed as mycoherbicide for the biocontrol of perennial sowthistle (*Sonchus arvensis* L.), produced a new chlorinated xanthone, methyl 8-hydroxy-3-methyl-4-chloro-9-oxo-9*H*-xanthene-1-carboxylate and a new benzophenone derivative, named 5-chloromoniliphenone, together with the already known 4-chloropinselin, methyl 3,8-dihydroxy-6-methyl-4-chloro-9-oxo-9*H*-xanthene-1-carboxylate, pinselin, methyl 3,8-dihydroxy-6-methyl-9-oxo-9*H*-xanthene-1-carboxylate, methyl 8-hydroxy-6-methyl-9-oxo-9*H*-xanthene-1-carboxylate, chloromonilicin, moniliphenone, chloromonilinic acids B-D, and α- and β-diversolonic esters (Berestetskiy et al., 2019; Dalinova et al., 2020).

The economical importance of mahogany wood, and then the need of deeper investigation on its diseases, together with the interest for phytotoxins produced by *Alternaria* species, prompted us to investigate the phytotoxins produced *in vitro* by *A. argyroxiphii*. Therefore, this manuscript reports the isolation and the chemical and biological characterization of nine specialized metabolites obtained from the liquid culture of *A. argyroxiphii*.

2. Results and Discussion

The organic extract of *A. argyroxiphii* was purified as reported in detail in the Experimental section to afford six already known phytotoxins, which were identified as porritoxinol (**4**), its closely

related phthalide **5**, its derivative **6**, zinniol (**7**), alternariol (**8**), and its 4-methyl ether (**9**) (Fig. 1), together with three new compounds: a trisubstituted dihydroisobenzofuranone (**1**), a tetrasubstituted 2-hydroxyethylbenzamide (**2**) and a tetrasubstituted phenyl dihydroxybutyl ether (**3**), named argyrotoxins A-C (**1**–**3**, Fig. 1).

Porritoxinol (**4**), its closely related phthalide **5**, its derivative **6**, zinniol (**7**), alternariol (**8**) and its 4-methyl ether (**9**) were identified by comparing their physical and spectroscopic data with those reported in literature. Data for **4** were already reported when its was isolated with the known tentoxin, porritoxin, and silvaticol from by *Alternaria porri*, the causal fungus of black spot disease in the stone-leek and onion (Suemitsu et al., 1994). Data for **5** were reported when it was isolated from the same fungus (Suemitsu et al., 1992). Data for **6** were reported when it was isolated from the endophytic fungus *Pestalotiopsis photiniae* Thüm (Yang et al., 2011). Previous data for **7** were reported by White and Starrat (1967) when it was isolated from *Alternaria zinniae*, which, as above cited, caused leaf and stem blight on zinnia, sunfloflower, and marigold. Data for compound **7** were also reported when it was isolated: i) as a phytotoxin from *Phoma macdonaldii* Boerema, the causal agent of stem blight of sunflower (*Helianthus annuus* L.) (Sugawara and Strobel, 1986); ii) as the main metabolite from *Alternaria tagetica* S.K. Shome & Mustafee, the causal agent of early blight in marigold (*Tagetes erecta* L.) (Gamboa-Angulo et al., 2000); iii) as phytotoxin isolated from *Alternaria cirsinoxia* E.G. Simmons & K. Mort (Berestetskii et al., 2010). Data for **8** and **9** were reported by Tan et al. (2008) when they were isolated together with a new alternariol derivative, 2240B and 4,10-dimethyl ether, from the mangrove endophytic fungus GYT of No. 2240 obtained from the South China Sea Coast. They showed strong anticancer activity against KB and KBv200 cells (Tan et al., 2008). Alternariol monomethyl ether (also named AME) (**9**), was previously isolated from an *Alternaria alternata* (Fr.) Keissl. strain isolated from grains of Linxian County, China, an area noted for a high incidence of esophageal cancer. Compound **9**

showed a strong mutagenic activity in *Escherichia coli* strain ND-160 (An et al., 1989). Both **8** and **9** were also previously isolated from the mycelium of *Alternaria dauci* (J.G. Kühn) J.W. Groves & Skolko (Freeman, 1966). The total synthesis of alternariol was also realized by Koch et al. (2005) in seven steps starting from orcinol and 3, 5-dimethoxybromobenzene. Further study on the mutagenicity of **8** and **9** in mammalian cells were also carried out (Brugger et al., 2006; Schrader et al., 2006).

The preliminary investigation carried out on argyrotoxins A-C (**1**–**3**) by ^{1}H and ^{13}C NMR analysis showed for **1** a carbon skeleton similar to that already observed in porritoxinol (**4**) and for **2** and **3** a structure similar to that of zinniol (**7**).

Argyrotoxin A (**1**) had a molecular formula of $C_{15}H_{18}O_6$ as deduced from its HR ESIMS, consistent with seven hydrogen deficiencies. Its IR (Nakanishi and Solomon, 1977) and UV spectra (Pretsch et al., 2000) showed the presence of bands typical of carboxylic, lactone, and aromatic moieties and absorption maxima indicating an extended conjugated system, respectively.

Its ^{1}H and COSY NMR spectra (Berger and Braun, 2004) (Table 1) showed the presence of two singlets at δ 7.07 and 5.37 typical of an aromatic proton (H-7) and of an oxygenated methylene (H$_2$C-3) probably involved in a lactone ring system. Furthermore, singlets at δ 3.88 and 2.19, due to a methoxy and a methyl groups were present together with those of a 3-substituted butyloxy side chain (Pretsch et al., 2000). This latter resulted to be a 3-carboxybutyloxy chain for the presence of a triplet ($J = 6.1$ Hz) at δ 4.09 (H$_2$C-1′), which in the COSY spectrum coupled with the two multiplets of the adjacent methylene group (H$_2$C-2′), which resonated at δ 2.27 and 1.98, respectively. The latter, in turn, coupled with the protons of the adjacent methine group (HC-3′) appearing as a broad quartet ($J = 7.0$ Hz) at δ 2.78. In fact, this proton (HC-3′) was also coupled with the adjacent methyl group (H$_3$C-5′), which resonated as a doublet ($J = 7.0$ Hz) at δ 1.30 (Pretsch et al., 2000). The final carboxyl group of this side chain resonated in the ^{13}C NMR spectrum as a singlet at δ 180.6 (Breitmaier and Voelter, 1987) and as

expected in the HMBC spectrum (Table 1) (Berger and Braun, 2004) coupled with the protons of the next methine (HC-3′), methyl (H₃C-5′) and methylene group (H₂C-2′). This side chain resulted to be located at C-6 of the pentasubstituted benzene ring system by the long range observed in the same spectrum between C-6 and H₂C-1'. Similarly, the methoxy and the methyl were located at C-4 and C-5 of the same ring system for the coupling observed between OMe and C-4 and for those of the methyl group with C-3a and C-6. The other carbonyl (O=C-1)group observed in ^{13}C NMR spectrum as a singlet at δ 171.5 belongs to a dihydrofuranone ring and significantly coupled in the HMBC spectrum H₂C-3. These latter protons (H₂C-3) also coupled in the same spectrum with C-4 and C-5 while the carbonyl (C-1) coupled with HC-7. Thus, the junction between the trisubstituted benzene and the dihydrofuranone rings resulted to be between C-3a and C-7a. Both these two tertiary sp^2 carbons coupled with HC-7, while C-7a also coupled with H₂C-3. Thus argyrotoxin A was constituted by a trisubstituted dihydrobenzofuranone ring system. The coupling observed in the HSQC spectrum (Berger and Braun, 2004) (Table 1) allowed to assign the chemical shifts to the protonated carbons. In particular, the signals observed at δ 101.6, 68.5, 66.5, 59.5, 36.4, 32.7, 17.3 and 9.8 were assigned to C-7, C-3, C-1′, OMe, C-3′, C-2′, C-5′ and MeC-5 (Breitmaier and Voelter, 1987). The signals observed at δ 159.2, 153.0, 128.4, 125.7, and 125.0 were assigned to tertiary sp^2 carbons C-6, C-4, C-7a, C-3a and C-5 on the basis of the coupling observed in the HMBC spectrum and reported in Table 1 (Breitmaier and Voelter, 1987). Thus the chemical shift were assigned to all the carbons and the corresponding protons as reported in Table 1 and argyrotoxin A (**1**) was formulated as 4-(7-methoxy-6-methyl-3-oxo-1, 3-dihydro-isobenzofuran-5-yloxy)-2-methyl-butyric acid. The structure assigned to **1** was supported from all the other coupling observed in the HMBC spectrum (Table 1) and from the data of its HR ESIMS spectrum which showed a sodium adduct ion [M + Na]$^+$ at *m/z* 317.1010. The ESIMS spectrum showed the same peak and the potassium [M + K]$^+$ and the protonated [M + H]$^+$ adduct ions at *m/z* 333 and 295. A significant

fragmentation ion $[M + H - H_2O]^+$ was generated from the protonated adduct ion by loss of H_2O at *m/z* 277. The correlation, observed in NOESY spectrum (Berger and Braun, 2004), between MeO and H_2C-3 and Me and HC-7 and H_2C-1' further supported the structure assigned to **1**.

Once determined the molecular structure of argyrotoxin A (**1**), a study to assign its absolute configuration was carried out. As inferred from Fig. S1 in the Supporting Information, the electronic circular dichroism (ECD) spectrum of **1** displayed a single weak negative Cotton effect at about 190 nm, while above 210 nm, only very weak signals ($\Delta\varepsilon < 0.01$) with a low signal to noise ratio were detected. This behavior was expected considering that the stereogenic center and the aromatic chromophoric moiety, absorbing in the 200–280 nm range, are far apart. Moreover, a preliminary molecular mechanics conformational analysis of compound **1** provided about 100 populated conformers within a 10 kcal/mol energy range. Such high molecular flexibility and the very weak chiroptical response of compound **1** prevented the direct application to this compound of the computational analysis of chiroptical data, the nowadays commonest method of choice for the absolute configuration assignment to natural (Superchi et al., 2018) and synthetic (Belviso et al., 2018) chiral compounds. Therefore, we resorted to the application of the so-called "chiroptical probes" for the absolute configuration assignment. These are achiral chromophoric moieties which, when linked to a chiral nonracemic substrate, give rise to diagnostic chiroptical signal(s), usually in ECD spectrum, from the sign of which the absolute configuration of the substrate can be determined without any computation. A very efficient type of chiroptical probes is constituted by the flexible 2,2′-bridged biphenyls, that we introduced some years ago. Such probes have been extensively used for the absolute configuration assignment to chiral diols (Superchi et al. 2001), carboxylic acids (Superchi et al., 2006; Vergura et al., 2019), and primary amines (Vergura et al., 2018), and recently applied to natural products (Santoro et al., 2020) and chiral drugs (Vergura et al., 2021). According this method 2-substituted carboxylic chiral acids, like compound **1**,

are transformed in the corresponding biphenylamides (Fig. 2), obtaining a pair of diastereomeric amides with opposite biphenyl twist. These distereomers are in a thermodynamic equilibrium and the most stable atropisomer is also the major one. Moreover, the sense of the biphenyl twist can be detected by the sign of ECD Cotton effect at 250 nm (biphenyl A band) (Sagiv et al., 1977), which is positive for a M torsion and negative for a P one (Mislow and Gordon, 1963). We demonstrated that for the absolute configuration depicted in Fig. 3 the diastereomer having P torsion is more stable (and thus more abundant) than the M twisted one (Superchi et al., 2006). Therefore, a non-empirical rule to determine the absolute configuration of chiral carboxylic acids by inspecting the sign of the biphenyl A band at ~250 nm in the ECD spectrum of their biphenylamides was established. According to such rule, a P biphenyl twist is preferred for 2-substituted aliphatic chiral carboxylic acids having absolute configuration such that a clockwise rotation leads from the largest to the smallest substituent on the acid moiety, and thus a negative A band is expected at around 250 nm in the ECD spectrum of the corresponding biphenyl derivatives. Vice versa, an M twist is preferred for a counterclockwise disposition of the substituents, and a positive A band arises in the ECD spectrum (Fig. 3).

To apply this method, argyrotoxin A (**1**) was then converted to the corresponding biphenylamide **1a** by reaction with the biphenylazepine 10 in the presence of EDC hydrochloride and N,N′-dimethylamminopyridine (DMAP) in CH_2Cl_2 (Fig. 4). The obtained biphenylamide **1a** was not purified but its UV and ECD spectra were directly recorded on the crude (Fig. 5). In fact, as reported above, we did not expect significant ECD signal interference from not reacted argyrotoxin A (**1**), being this almost ECD silent, while racemic amine 10 was not ECD active as well. Therefore, the only ECD active compound was the biphenylamide derivative **1a**. The UV spectrum of **1a** showed the typical features of the biphenyl chromophore, with the A band at about 240 nm and the more intense C band at about 200 nm (Sagiv et al., 1977). In the ECD spectrum, a positive Cotton effect was visible at 236 nm and a

negative one at 224 nm. At shorter wavelength, the higher UV absorbance, due also to unreacted biphenylazepine 10, prevented detection of clear ECD signals. The positive Cotton effect in correspondence to the biphenyl A band revealed an M twist of the biphenyl moiety in **1a**, then allowing to assign (*R*) absolute configuration to the C-3' stereocenter on the basis of the mnemonic rule depicted in Fig. 3.

Argyrotoxin B (**2**) had a molecular formula of $C_{17}H_{24}O_6$ as deduced from its HR ESIMS spectrum which was consistent with six hydrogen deficiencies. Its IR (Nakanishi and Solomon, 1977) spectrum (Pretsch et al., 2000) showed the presesence of bands typical of hydroxy, carbonyl, olefinic and aromatic residues, while the UV spectrum showed absortion maxima typical for aromatic systems.

Its 1H NMR and COSY spectra (Table 2) showed a singlet δ 7.08 typical of a pentasubstituted benzene ring proton (H-5) and three singlets at δ 4.53, 3.86, 2.20 typical of a benxylic hydroxymethylene, a methoxy and a methyl groups (Pretsch et al., 2000). Furthermore, the signal systems of two side chains were also analyzed. The first was a 3-methylbut-2-enyloxy, as deduced from the doublet ($J = 6.8$ Hz) of an oxygenated methylene group (H_2C-1′) resonating at δ 4.57 which coupled with the broad triplet ($J = 6.8$ Hz) of the adjacent proton (HC-2′) of a trisubstituted olefinic group at δ 5.50. The latter proton (HC-2′) was also allylic coupled ($J < 1$ Hz) with the two methyl groups (Me-5' and Me-4') of the tail observed at δ 1.79 and 1.74, respectively (Sternhell, 1969; Pretsch et al., 2000). The other side chain showed signal system typical of a 2-hydroxyethylcarboxyamide, appearing as two coupled triplet ($J = 4.8$ Hz) at δ 3.92 (H_2C-2″) and 3.77 (H_2C-1″). The carbonyl group of this residue resonated in the ^{13}C NMR spectrum (Table 2) at δ 170.2 and coupled in the HMBC spectrum (Table 2) with H_2C-2″ as well as with CH_2OH and H-5. The latter correlation permitted to locate it at C-6 of benzene ring. The coupling observed in the same spectrum between the OMe and C-4 and between Me and C-2, C-3, C-4 and C-6 allowed to locate these groups at C-2 and C-3, respectively. Consequently,

the 3-methylbut-2-enyloxy residue resulted to be located at C-4. The coupling observed the HSQC spectrum allowed to assign the protonated carbons. In particular, the signals observed at δ 119.8, 101.4, 65.9, 62.2, 59.9, 50.2, 46.7, 25.9, 18.4 and 9.7 were assigned to C-2′ , C-5, C-1′ , C-2″ , OMe, CH₂OH, C-1″ C-4′ , C-5′ and Me (Breitmaier and Voelter, 1987). The tertiary sp² olefinic carbon C-3' was assigned to the signal at δ 137.9 by the couplings observed in the HMBC spectrum with H₂C-1', Me-4' and Me-5'. The five tertiary sp² aromatic carbons at δ 158.8, 153.5, 131.7, 124.1 and 123.5 coupled, respectively, with Me, OMe and Me, Me and CH₂OH, H-5, Me and CH₂OH, and Me and CH₂OH and were assigned to C-2, C-4, C-6, C-1 and C-3. (Breitmaier and Voelter, 1987). Thus the chemical shifts were assigned to all the carbons and corresponding protons as reported in Table 2 and agyrotoxin B (**2**) was formulated as 5-but-2-enyloxy-N-(2-hydroxy-ethyl)-2-hydroxymethyl-3-methoxy-4-methyl-benzamide. The structure assigned to **2** was supported by all the other couplings observed in the HMBC spectrum (Table 2) and from the data of its HR ESI MS spectrum which showed the peak generated from its sodiated adduct ion by loss of H_2O $[M + Na - H_2O]^+$ at *m/z* 328.1534. The ESI MS spectrum the same peak and the ions generated by loss of H_2O from the potassium and protonated adduct ions $[M + K - H_2O]^+$ and $[M + H - H_2O]^+$ at *m/z* 344 and 306. The correlations observed in the NOESY spectrum (Berger and Braun, 2004) between OMe and CH₂OH, this latter and H₂C-1″ , H-5 and H₂C-1', H₂-2' with both Me-4′ and Me-5' and between these latter two methyl groups further supported the structure assigned to **2**.

Agryrotoxin C (**3**) had a molecular formula of $C_{16}H_{26}O_6$ has deduced from its HR ESIMS spectrum and consistent with four hydrogen deficiencies. Its IR spectrum (Nakanishi and Solomon, 1977) showed the presesence of bands typical of hydroxy and aromatic residues, while the UV spectrum showed absortion maxima typical for aromatic systems (Pretsch et al., 2000).

The preliminary investigation of its ^{1}H and ^{13}C NMR spectra showed that it was close to both zinniol (**7**) and agyrotoxin B (**2**) bearing a tetrasubstituted anisole moiety as those compouds. However, **3** differed from **7** for the presence of a methoxymethylene group and of the side chains attached to C-1, C-4 and C-6. In fact, its ^{1}H and COSY (Table 2) spectra showed a singlet typical of another methoxy group at δ 3.39 which was linked, on the basis of the coupling observed in the HMBC (Table 2) to the benzylic methylene at C-1, which resonated as singlet at δ 4.53. The same spectra showed, as in **7**, the singlet of the other benzyl hydroxymethylene group at δ 4.68 linked at C-6. Futhermore, the side chain located to C-4, that in **7** was a 3-methylbut-2-enyloxy, in **3** was a 2,3-dihydroxy-3-methylbutyloxy. In fact, the ^{1}H and COSY spectra showed the presence of three doublet doublets typical of an ABC system (J = 9.8 and 3.3 and J = 9.8 and 8.0 Hz and J = 8.0 and 3.3) for the signal of H$_2$C-1′ and HC-2′ observed at δ 4.29 and 3.98 and 3.78 respectively (Sternhell, 1969). The two singlets of the two terminal methyl groups (Me-4' and Me-5'), resonating at δ 1.29 and 1.26, were linked C-3′ by their couplings as observed the HMBC spectrum (Table 2). C-3' in the same spectrum also coupled with the proton of the adjacent hydroxylated methine HC-2', which resonated in the ^{13}C NMR spectrum at δ 72.8 (Breitmaier and Voelter 1987).

The coupling observed in the HSQC and the HMBC spectra allowed to assign the chemical shifts to all the carbons and corresponding protons and argyrotoxin C (**3**) was formulated as 1-(5-(hydroxymethyl)-3-methoxy-4-(methoxymethyl)-2-methyl-phenoxy)-3-methylbutane-2,3-diol.

The structure assigned to **3** was supported the data of its HR ESIMS spectrum which showed the sodiated adduct ion [M + Na]$^+$ at *m/z* 337.1635. The ESI MS showed the same peak and the dimer potassium adduct ion [2M + K]$^+$ at *m/z* 353 and a significat fragmentation ion, generated by the protonated adduct ion by loss of MeOH [M + H – MeOH]$^+$ at *m/z* 283.

Among the metabolites isolated from *A. argyroxiphii* (**1**–**9**), zinniol (**7**) appeared to be the most active metabolite. As shown in Table 3, zinniol (**7**) caused necrotic lesions (necrosis area ranging from 7.1 to 77.5 mm^2) to leaves of all species tested. Toxic effects were also observed for argyrotoxin A (**1**) and B (**2**) only on leaves of bean, while porritoxinol (**4**) was active only on holm oak leaves. The other metabolites (**3**, **5**, **6**, **8** and **9**) appeared to be not phytotoxic on all species plants tested. This could also be dependent from the different plant sensitivity.

The results obtained suggested some structure-activity relationships. The substituents of the benzene ring of zinniol (**7**) are important features for the activity. In fact, when the hydroxymethylene at C-6 was oxidized to a carboxylic group and this, in turn, converted into the corresponding 2-hydroxyethylamide the activity decreased as observed in argyrotoxin B (**2**). Also the 3-methylbut-2-enyloxy chain at C-4 plays a role as its modification determined the loss of activity as in argyrotoxin C (**3**). In the porritoxinol group of metabolites (**1**, **4**–**6**) the two ortho-hydroxymethylene groups were converted in the furanone ring, and a compound selectivity was observed, as porritoxinol (**4**) and argyrotoxin A (**1**) were the only toxic compounds but on two different tested plants. This could depend from the butyloxy side chain at C-6, which, although have the same flexibility was differently fuctionalized in **4** in respect to **1**. The same residue at C-6 was converted into but-2-enyloxy differently funzionalized in **5** and **6** generating the loss of activity. The two tetrasubstituted benzochromenones **8** and **9**, having no structural correlation with either zinniol (**7**) or porritoxinol (**4**) were completely inactive.

3. Conclusions

Three previously undescribed phytotoxic compunds, named argyrotoxins A-C (**1**–**3**) were isolated from *A. argyroxiphii*, the causal agent of leaf spots on African mahogany trees (*Khaya*

senegalensis). The (3'*R*) absolute configuration was assigned to argyrotoxin A (**1**) by applying a flexible biphenyl as "chiroptical probe". Furthermore, porritoxinol (**4**), its closely related phthalide **5**, zinniol (**7**), alternariol (**8**), and its 4-methyl ether (**9**) were identified for the first time as toxins produced by this fungus. These are all already known metabolites belonging to well known classes of natural compounds and previously also isolated as fungal phytotoxins (Turner and Aldridge 1983; Cimmino et al., 2015; Masi et al., 2018a, 2018b; *Masi and Evidente, 2020*). Some of them are known as *Alternaria* toxins, such as porritoxinol (**4**) and closely related phthalide **5**, coming from *A. porri* (Suemitsu et al., 1994), zinniol (**7**) from *A. zinniae* (White and Starrat, 1967), *A. tagetica* (Gamboa-Angulo et al., 2000) and *A. cirsinoxia* (Berestetskii et al., 2010), alternariol (**8**) and its 4-methyl ether (**9**) from *A. dauci* (Freeman, 1966) and *A. alternata* (An et al., 1989).

4. Experimental section

4.1. *General Experimental Procedures*

Optical rotations were measured in a MeOH solution on a Jasco P- 1010 digital polarimeter; Infrared (IR) spectra were recorded as a glassy film on a PerkinElmer Spectrum One Fourier Transform Infrared (FTIR) spectrometer. Ultraviolet (UV) spectra were recorded on a JASCO V-530 spectrophotometer in CH_3CN solution. ECD spectra were recorded with a Jasco J-815 spectropolarimeter. ^1H and ^{13}C NMR spectra were recorded at 400 and 100 MHz, respectively, in $CDCl_3$ on a Bruker spectrometer. The same solvent was used as an internal standard. Carbon multiplicities were determined by DEPT spectra (Berger and Braun, 2004) DEPT, COSY-45, HSQC, HMBC and NOESY experiments (Berger and Braun, 2004) were performed using Bruker microprograms. HRESI and ESI mass spectra and liquid chromatography (LC)/MS analyses were performed using the LC/MS TOF system Agilent 6230B, HPLC 1260 Infinity. The HPLC separations were performed with a Phenomenex

LUNA (C18 (2) 5 µ 150 × 4.6 mm. Analytical and preparative TLC was performed on silica gel plates (Merck, Kieselgel 60, F_{254}, 0.25 and 0.5 mm respectively) or on reverse phase (Whatman, KC18 F_{254}, 0.20 mm) plates and the compounds were visualized by exposure to UV light and/or iodine vapors and/or by spraying first with 10 % H_2SO_4 in MeOH, and then with 5 % phosphomolybdic acid in EtOH, followed by heating at 110 ◦C for 10 min. CC: silica gel (Merck, Kieselgel 60, 0.063–0.200 mm). Biphenylazepine (10) was prepared as previously described (Superchi et al., 2006).

4.2. Fungal material

The *A. argyroxiphii* E.G. Simmons & Aragaki strain (CBS 117222), used in this study was purchased from Westerdijk Fungal biodiversity Intitute, Utrecht, Netherlands. Pure cultures were maintained on carrotagar and stored at 4 ◦C in the collection of the Dipartimento di Agraria, University of Sassari, Italy.

4.3. Production and isolation

The fungus was grown on liquid medium (Czapek amended with 2 % yeast extract and malt aextract; pH 5.7). The culture filtrates (5 L) were extracted exhaustively with EtOAc at pH 4.0, yielding an oily brown residue (1.4 g). This latter was fractionated by CC eluted with $CHCl_3$-*iso*-PrOH (9:1) yielding nine groups of homogeneous fractions F1–F9. The residue of F2 (63.2 mg) was purified on preparative TLC eluted by *n*-hexane-EtOAc (7:3) yielding 6-(3′,3′-dimethyallyloxy)-4-methoxy-5-methylphthalide (**5**, 7.3 mg) as an amorphous solid and alternariol methyl ether (9, 4.5 mg) as white solid. The residue of F3 (108.5 mg) was purified by CC eluted with $CHCl_3$-acetone (8:2) obtaining six fractions F3.1-F3.6. The residue of F3.2 (10.0 mg) was purified on TLC eluted with $CHCl_3$–MeOH (95:5) yielding zinniol (**7**, 4.1 mg) as an amorphous solid. The residue of F3.3 (35.3 mg) was purified on preparative TLC using

petroleum ether-acetone (7:3), obtaining further amount of zinniol (**7**, 4.6 mg, for a total of 8.7 mg) and porritoxinol (**4**, 17.4 mg) as an amorphous solid. The residue of F3.4 (43.7 mg) was purified on preparative TLC eluted with $CHCl_3$–MeOH (9:1) yielding alternariol (**8**, 15.0 mg) as an amorphous solid. The residue of F4 (32.4 mg) was purified by reverse phase TLC using $MeCN$–H_2O (7:3) as eluent, obtaining argyrotoxin C (**3**, 2.7 mg) as a yellow oil. The residue of F5 (32.6 mg) was further purified by preparative TLC eluting with $CHCl_3$–MeOH (9:1) obtaining argyrotoxin B (**2**, 1.9 mg) as an amorphous solid. The residue of F6 (64.7 mg) was further purified by preparative TLC eluted with $CHCl_3$-*iso*-PrOH (95:5) obtaining argyrotoxin A (**1**, 3.5 mg) as an amorphous solid. The residue of F8 (36.6 mg) was purified by preparative TLC eluted with $CHCl_3$–MeOH (9:1), yielding the phthalide derivative (**6**, 10.0 mg).

4.3.1. *Argirotoxin A (1)*

Amorphous solid; UV λ_{max} nm (log ε) 298 (3.2), 254 (3.6); IR ν_{max} 3400, 1754, 1700, 1618, 1466, 1423, 1125 cm^{-1}; ^{1}H and ^{13}C NMR, see Table 1; (+)-HR ESIMS: *m/z* 317.1010 [M + Na]$^+$ (calcd for $C_{15}H_{18}NaO_6$, 317.1001); (+)-ESIMS 333 [M + K]$^+$, 317 [M + Na]$^+$, 295 [M + H]$^+$ and 277 [M + H - H_2O]$^+$.

4.3.2. *Argirotoxin B (2)*

Amorphous solid; UV λ_{max} nm (log ε) 291 (3.3), 254 (3.7); IR ν_{max} 3409, 1660, 1620, 1561, 1453, 1424, 1124 cm^{-1}; ^{1}H and ^{13}C NMR, see Table 2; (+)-HR ESIMS *m/z*: 328.1534 [M + Na - H_2O +]$^+$ (calcd for $C_{17}H_{23}NNaO_4$ 328.1525); (+)-ESIMS *m/z*: 344 [M + K - H_2O]$^+$, 328 [M + Na - H_2O]$^+$ 306 [M - H_2O + H]$^+$.

4.3.3. *Argirotoxin C (3)*

Amorphous solid; UV λ_{max} nm (log ε) 273 (3.2); IR ν_{max} 3369, 1605, 1582, 1456, cm^{-1}; ^{1}H and ^{13}C

NMR, see Table 2; (+)-HR ESIMS m/z: 337.1635 [M + Na]$^+$ (calcd for $C_{16}H_{26}NaO_6$ 337.1627); (+)-

ESIMS m/z: 353 [2M + K]$^+$, 337 [M + Na]$^+$, 283 [M + H – MeOH]$^+$.

4.3.4. Synthesis of biphenylamide 1a

To a solution of the biphenylazepine 10 (1.25 equiv.) in anhydrous CH_2Cl_2 were added, in

sequence, compound **1** (1 equiv., 0.05 M), 1-[3-(dimethylamino)propyl]-3-ethylcarbodiimide

hydrochloride (EDC.HCl) (1.7 equiv.), and N,N′-dimethylamino pyridine (DMAP) (1 equiv.). The

resulting solution was stirred overnight at rt, then diluted with CH_2Cl_2, washed with 10 % aqueous

$NaHCO_3$, brine, and dried over anhydrous Na_2SO_4. After evaporation of solvent the recovered residue

was used without further purification. The UV and ECD spectra of **1a** mixture were recorded in CH_3CN

solution in the 180–350 nm range.

4.4. Phytotoxic assay

All compounds (**1**–**9**) were tested by leaf puncture assay using bean (*Phaseolus vulgaris* L.), English

ivy (*Hedera helix* L.) and holm oak (*Quercus ilex* L.) young leaves. Each compound was tested at 1.0

mg/mL. Compounds were first dissolved in MeOH, and then a stock solution with sterile distilled water

was prepared. A droplet (20 μL) of test solution was applied on the adaxial sides of leaves that had

previously been needle punctured. Droplets (20 μL) of MeOH in distilled water (4 %) were applied on

leaves as negative control. Each treatment was repeated three times. Leaves were observed daily and

scored for symptoms after 10 days. The effect of the toxins on the leaves was observed up to 15 days.

Lesions were estimated using APS Assess 2.0 software following the tutorials in the user's manual. The

lesion size was expressed in mm^2.

Declaration of competing interest

The authors declare that they have no known competing financial interests or personal relationships that could have appeared to influence the work reported in this paper.

Acknowledgments

Appendix A. Supplementary data

Supplementary data to this article can be found online at https://doi.org/10.1016/j.phytochem.2021.112921.

References

An, Y., Zhao, T., Miao, J., Liu, G., Zheng, Y., Xu, Y., Van Etten, R.L., 1989. Isolation, identification, and mutagenicity of alternariol monomethyl ether. J. Agric. Food Chem. 37, 1341–1343.

Becker, A.M., Richards, R.W., Schmalzl, K.J., Yick, H.C., 1978. Metabolites of *Dactylaria lutea*. J. Antibiot. (Tokyo) 31, 324–329.

Belviso, S., Santoro, E., Lelj, F., Casarini, D., Villani, C., Franzini, R., Superchi, S., 2018. Stereochemical stability and absolute configuration of atropisomeric alkylthioporphyrazines by dynamic NMR and HPLC studies and computational analysis of HPLC-ECD recorded spectra. Eur. J. Org Chem. 4029–4037, 2018.

Berestetskii, A.O., Yuzikhin, O.S., Katkova, A.S., Dobrodumov, A.V., Sivogrivov, D.E., Kolombet, L.V., 2010. Isolation, identification, and characteristics of the phytotoxin produced by the fungus *Alternaria cirsinoxia*. Appl. Biochem. Microbiol. 46, 75–79.

Berestetskiy, A.O., Dalinova, A.A., Volosatova, N.S., 2019. Metabolite profiles and biological activity of extracts from *Alternaria sonchi* S-102 culture grown by different fermentation methods. Appl. Biochem. Microbiol. 55, 284–293.

Berger, S., Braun, S., 2004. 200 and More Basic NMR Experiments: a Practical Course, first ed. Wiley-VCH, Weinheim.

Breitmaier, E., Voelter, W., 1987. Carbon-13 NMR Spectroscopy. VCH, Weinheim.

Brugger, E.M., Wagner, J., Schumacher, D.M., Koch, K., Podlech, J., Metzler, M., Lehmann, L., 2006. Mutagenicity of the mycotoxin alternariol in cultured mammalian cells. Toxicol. Lett. 164, 221–230.

Cimmino, A., Masi, M., Evidente, M., Superchi, S., Evidente, A., 2015. Fungal phytotoxins with potential herbicidal activity: chemical and biological characterization. Nat. Prod. Rep. 32, 1629–1653.

Couto, J.M.F., Otoni, W.C., Pinheiro, A.L., Fonseca, E.P., 2004. Desinfestaç˜ao e germinaç˜ao in vitro de sementes de mogno (*Swietenia macrophylla* King). Rev. ´Arvore 28, 633–642.

Dalinova, A., Chisty, L., Kochura, D., Garnyuk, V., Petrova, M., Prokofieva, D., Yurchenko, A., Dubovik, V., Ivanov, A., Smirnov, S., Zolotarev, A., Berestetskiy, A., 2020. Isolation and bioactivity of secondary metabolites from solid culture of the fungus *Alternaria sonchi*. Biomolecules 10, 81.

Falesi, I.C., Baena, A.R.C., 1999. Mogno africano Khaya ivorensis A. Chev. em sistema silvipastoril com leguminosa e revestimento natural do solo. Embrapa Amazˆonia Oriental, Bel´em, p. 52.

Freeman, G.G., 1966. Isolation of alternariol and alternariol monomethyl ether from *Alternaria dauci* (kühn) groves and skolko. Phytochemistry 5, 719–725.

Gamboa-Angulo, M.M., Alejos-Gonz´alez, F., Escalante-Erosa, F., García-Sosa, K., Delgado-Lamas, G., Pe˜na-Rodríguez, L.M., 2000. Novel dimeric metabolites from *Alternaria tagetica*. J. Nat. Prod. 63, 1117–1120.

Gasparotto, L., Hanada, R.E., Albuquerque, F.C., Duarte, M.L.R., 2001. Mancha areolada causada por *Thanatephorus cucumeris* em mogno-africano. Fitopatol. Bras. 26, 660–661.

Koch, K., Podlech, J., Pfeiffer, E., Metzler, M., 2005. Total synthesis of alternariol. J. Org. Chem. 70, 3275–3276.

Masi, M., Evidente, A., 2020. Fungal bioactive anthraquinones and analogues. Toxins 12,714.

Masi, M., Cimmino, A., Reveglia, P., Mugnai, L., Surico, G., Evidente, A., 2018b. Advances on fungal phytotoxins and their role in grapevine trunk diseases. J. Agric. Food Chem. 66, 5948–5958.

Masi, M., Maddau, L., Linaldeddu, B.T., Scanu, B., Evidente, A., Cimmino, A., 2018a. Bioactive metabolites from pathogenic and endophytic fungi of forest trees. Curr. Med. Chem. 25, 208–252.

Mislow, K., Gordon, A.J., 1963. Photoracemization of biphenyls. J. Am. Chem. Soc. 85, 3521-3521.

Nakanishi, K., Solomon, P.H., 1977. Infrared Absorption Spectroscopy, second ed. Holden Day, Oakland, pp. 17–44.

Pinheiro, A.L., Couto, L., Pinheiro, D.T., Brunetta, J.M.F.C., 2001. Ecologia, silvicultura e tecnologia de utilizaç˜ao dos mognos-africanos (Khaya spp.). Viçosa, UFV, p. 102.

Pontes, J.G.D.M., Fernandes, L.S., dos Santos, R.V., Tasic, L., Fill, T.P., 2020. Virulence factors in the phytopathogen–host interactions: an overview. J. Agric. Food Chem. 68, 7555–7570.

Pretsch, E., Bühlmann, P., Affolter, C., 2000. Structure Determination of Organic Compounds – Tables of Spectral Data, third ed. Springer-Verlag, Berlin, pp. 161–243.

Sagiv, J., Yogev, A., Mazur, Y., 1977. Application of linear dichroism to the analysis of electronic absorption spectra of biphenyl, fluorene, 9,9'-spirobifluorene, and [6.6] vespirene. Interpretation of the circular dichroism spectrum of [6.6]vespirene. J. Am. Chem. Soc. 99, 6861–6869.

Santoro, E., Vergura, S., Scafato, P., Belviso, S., Masi, M., Evidente, A., Superchi, S., 2020. Absolute configuration assignment to chiral natural products by biphenyl chiroptical probes: the case of the phytotoxins colletochlorin A and agropyrenol. J. Nat. Prod. 83, 1061–1068.

Schrader, T.J., Cherry, W., Soper, K., Langlois, I., 2006. Further examination of the effects of nitrosylation on *Alternaria alternata* mycotoxin mutagenicity in vitro. Mutat. Res. Genet. Toxicol. Environ. Mutagen 606, 61–71.

Simmons, E.G., 2007. Alternaria: an Identification Manual. CBS Fungal Biodiversity Centre, Utrecht, Netherlands. Sternhell, S., 1969. Q. Rev. 23, 236–270.

Stoessl, A., Unwin, C.H., Stothers, J.B., 1979. Metabolites of Alternaria solani part V. Biosynthesis of altersolanol A and incorporation of altersolanol A-13Cx into altersolanol B and macrosporin. Tetrahedron Lett. 27, 2481–2484.

Strobel, G.A., 1982. Phytotoxins. Annu. Rev. Biochem. 51, 309–333.

Suemitsu, R., Kitagawa, N., Horie, S., Kazawa, K., Harada, T., 1978. Isolation and identification of altersolanol B (7-methoxy-2-methyl-(2R,3S)-1,2,3,4-tetrahydro-2,3,5-trihydroxyanthraquinone) from the mycelium of *Alternaria porri* (ellis) ciferri. Agric. Biol. Chem. 42, 1801–1802.

Suemitsu, R., Ohnishi, K., Horiuchi, M., Morikawa, Y., 1992. Isolation and identification of 6-(3',3'-dimethylallyloxy)-4-methoxy-5-methylphthalide from *Alternaria porri*. Biosci. Biotechnol. Biochem. 56, 986-986.

Suemitsu, R., Ohnishi, K., Morikawa, Y., Ideguchi, I., Uno, H., 1994. Porritoxinol, a phytotoxin of *Alternaria porri*. Phytochemistry 35, 603–605.

Sugawara, F., Strobel, G., 1986. Zinniol, a phytotoxin, is produced by Phoma macdonaldii. Plant Sci. 43, 19–23.

Superchi, S., Bisaccia, R., Casarini, D., Laurita, A., Rosini, C., 2006. Flexible biphenyl chromophore as a circular dichroism probe for assignment of the absolute configuration of carboxylic acids. J. Am. Chem. Soc. 128, 6893–6902.

Superchi, S., Scafato, P., Gorecki, M., Pescitelli, G., 2018. Absolute configuration determination by quantum mechanical calculation of chiroptical spectra: basics and applications to fungal metabolites. Comput. Mater. Continua (CMC) 25, 287–320.

Tan, N., Tao, Y., Pan, J., Wang, S., Xu, F., She, Z., Jones, E.G., 2008. Isolation, structure elucidation, and mutagenicity of four alternariol derivatives produced by the mangrove endophytic fungus No. 2240. Chem. Nat. Compd. 44, 296–300.

Teixeira, L.P., Soares, T.D.P.F., Oliveira, L.S.S., Mathioni, S., Ferreira, M.A., 2017. First report of leaf spot caused by *Alternaria argyroxiphii* on African mahogany trees (*Khaya senegalensis*). Phytopathol. Mediterr. 56, 502–510.

Turner, W.B., Aldridge, D.C., 1983. Fungal Metabolites II. Academic Press, London.

Vergura, S., Pisani, L., Scafato, P., Casarini, D., Superchi, S., 2018. Central-to-axial chirality induction in biphenyl chiroptical probes for the stereochemical characterization of chiral primary amines. Org. Biomol. Chem. 16, 555–565.

Vergura, S., Scafato, P., Belviso, S., Superchi, S., 2019. Absolute configuration assignment from optical rotation data by means of biphenyl chiroptical probes. Chem. Eur J. 25, 5682–5690.

Vergura, S., Orlando, S., Scafato, P., Belviso, S., Superchi, S., 2021. Absolute configuration sensing of chiral aryl- and aryloxy-propionic acids by biphenyl chiroptical probes. Chemosensors 9, 154.

Woudenberg, J.H.C., Groenewald, J.Z., Binder, M., Crous, P.W., 2013. Alternaria redefined. Stud. Mycol. 75, 171–212.

White, G.A., Starrat, A.N., 1967. The production of a phytotoxic substance by *Alternaria zinniae*. Can. J. Bot. 45, 2087–2090.

Yang, X.L., Zhang, S., Hu, Q.B., Luo, D.Q., Zhang, Y., 2011. Phthalide derivatives with antifungal activities against the plant pathogens isolated from the liquid culture of *Pestalotiopsis photiniae*. J. Antibiot. 64, 723–727.

Table 1 . ¹H and ¹³C NMR Data of Argirotoxin A (1)[a,b]

No.	δ_C[c]	δ_H (J in Hz)	HMBC
1	171.5 s		H$_2$-3, H-7
2			
3	68.5 t	5.37 s (2H)	
3a	125.7 s		Me, H-7
4	153.0 s		Me, Me, H$_2$-3, H-7
5	125.0 s		H$_2$-3
6	159.2 s		Me, H-7, H$_2$-1'
7	101.6 d	7.07 s	
7a	128.4 s		H$_2$-3, H-7
1'	66.5 t	4.09 t (6.1) (2H)	H$_2$-2'
2'	32.7 t	2.27 m	H$_2$-1', H-3', H$_3$-5'
		1.98 m	
3'	36.4 d	2.78 q (7.0)	H$_2$-1', H$_2$-2', H$_3$-5'
4'	180.6 s		H$_2$-2', H-3', H$_3$-5'
5'	17.3 q	1.30 d (7.0) (3H)	H$_2$-2', H-3'
OMe	59.5 q	3.88 s	
Me	9.8 q	2.19 s	

[a]The chemical shifts are in δ values (ppm) from TMS.[b]2D ¹H, ¹H (COSY) and ¹³C, ¹H (HSQC) NMR experiments confirmed the correlations of all the protons and the corresponding carbons. [c]Multiplicities were assigned with DEPT.

Table 2. ^{1}H and ^{13}C NMR Data of Argirotoxin B and C (2 and 3)^{a,b}

No.	$\delta_C{}^c$	δ_H (*J* in Hz)	HMBC	$\delta_C{}^c$	δ_H (*J* in Hz)	HMBC
		2			**3**	
1	124.1 s		H-5, Me, CH$_2$OH	121.7 s		OCH$_2$, CH$_2$OMe, H-5
2	158.8 s		Me	159.7 s		OMe, Me, CH$_2$OMe
3	123.5 s		Me, CH$_2$OH	119.5 s		Me, H-5
4	153.5 s		MeO, Me	159.5 s		Me, H-5
5	101.4 d	7.08 s		108.1 d	6.91 s	OCH$_2$
6	131.7 s		Me, CH$_2$OH	141.7 s		OCH$_2$, CH$_2$OME
1'	65.9 t	4.57 d (6.8) (2H)		70.8 t	4.29 dd (9.8, 3.3) 3.98 dd (9.8, 8.0)	
2'	119.8 d	5.50 br t (6.8)	H$_2$-1', Me-4', Me-5'	77.7 d	3.78 dd (8.0, 3.3)	Me-4', Me-5', H-1'B
3'	137.9 s		H$_2$-1', Me-4', Me-5'	72.8 s		H-2', Me-4', Me-5'
Me-4'^{d}	25.9 q	1.79 br s	Me-5'	26.7 q	1.29 s	Me-5'
Me-5'^{d}	18.4 q	1.74 br s	Me-4'	25.0 q	1.26 s	H-2', Me-4'
1"	46.7 t	3.77 t (4.8) (2H)	H$_2$-2"			
2"	62.2 t	3.92 t (4.8) (2H)				
OMe	59.9 q	3.86 s		62.3 q	3.73 s	
OCH$_2$	50.2 t	4.53 s		62.6 t	4.68 s	H-5
CH$_2$OMe				58.2 t	3.39 s	CH$_2$OMe
CH$_2$OMe				66.7 q	4.53 s	CH$_2$OMe
Me	9.7 q	2.20 s		9.4 q	2.18	
C=O	170.2 s		H-5, H$_2$-2", CH$_2$OH			

^{a}The chemical shifts are in δ values (ppm) from TMS. ^{b}2D ^{1}H, ^{1}H (COSY) and ^{13}C, ^{1}H (HSQC) NMR experiments confirmed the correlations of all the protons and the corresponding carbons. ^{c}Multiplicities were assigned with DEPT. ^{d}These assignment could be reversed.

Table 3. Phytotoxicity data for compounds 1–9 produced *in vitro* by *Alternaria argyroxiphii* tested at 1 mg/mL.

Compound	Leaf puncture bioassay^a		
	Bean	English ivy	Holm oak
1	6.7 ± 1.1	na^b	na
2	7.7 ± 1.1	na	na
3	na	na	na
4	na	na	16.7 ± 3.2
5	na	na	na
6	na	na	na
7	77.5 ± 6.4	12.9 ± 1.5	7.1 ± 0.6
8	na	na	na
9	na	na	na

^{a}Data are expressed as median area lesion ± error standard (mm^2).
^{b}na = inactive.

Figure Legend

Figure 1. Chemical structures of compounds **1–9**.

Figure 2. Biphenyl probes for the absolute configuration determination to chiral acids by ECD. L = largest group, M = medium size group, S = smallest group.

Figure 3. Mnemonic scheme relating the absolute configuration and the sign of the A band in the ECD spectrum of biphenylamides. L = largest group, M = medium size group, S = smallest group.

Figure 4. Synthesis of biphenylamide **1a** from argyrotoxin A (**1**).

Figure 5. UV and ECD spectra (CH_3CN) of biphenylamide **1a**. Being the spectra recorded on crude mixture, values on vertical axes are on arbitrary units.

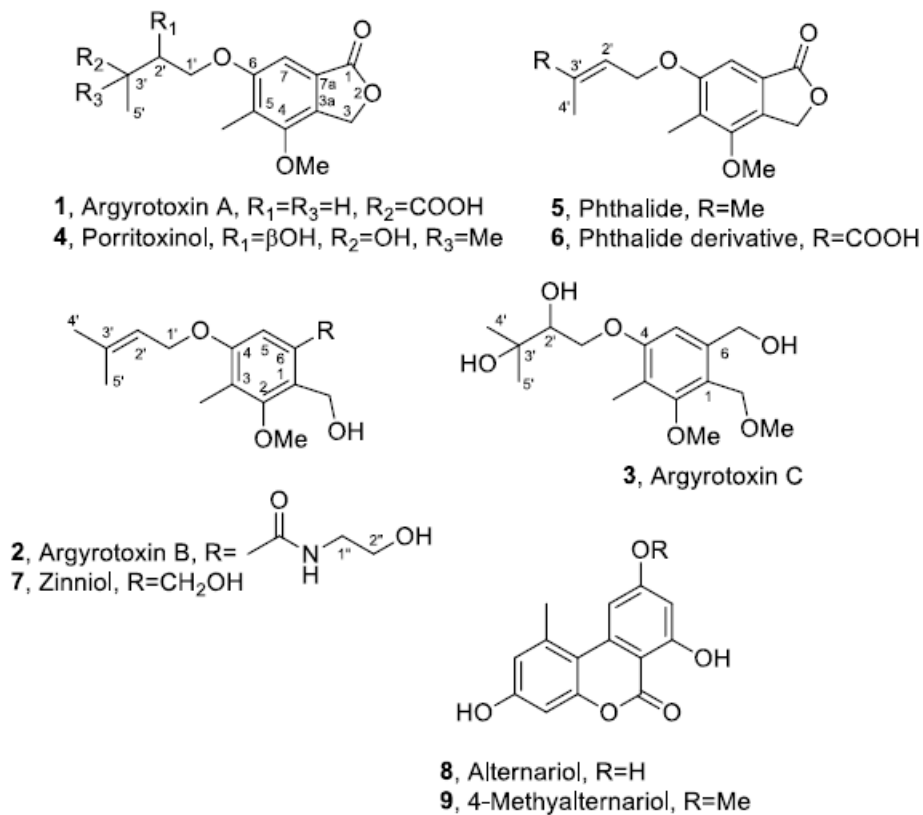**Fig. 1. Chemical structures of compounds 1–9.**

1, Argyrotoxin A, R$_1$=R$_3$=H, R$_2$=COOH
4, Porritoxinol, R$_1$=βOH, R$_2$=OH, R$_3$=Me

5, Phthalide, R=Me
6, Phthalide derivative, R=COOH

3, Argyrotoxin C

2, Argyrotoxin B, R=
7, Zinniol, R=CH$_2$OH

8, Alternariol, R=H
9, 4-Methyalternariol, R=Me

Fig. 2. Biphenyl probes for the absolute configuration determination to chiral acids by ECD. L = largest group, M = medium size group, S = smallest group.

10

negative ECD A band
at 250 nm
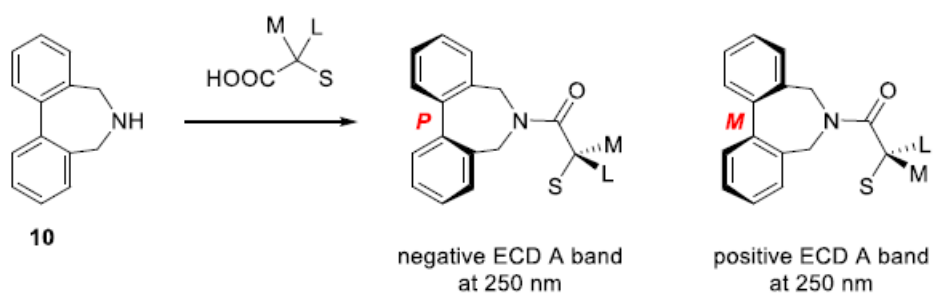
positive ECD A band
at 250 nm

Fig. 3. Mnemonic scheme relating the absolute configuration and the sign of the A band in the ECD spectrum of biphenylamides. L = largest group, M = medium size group, S = smallest group.
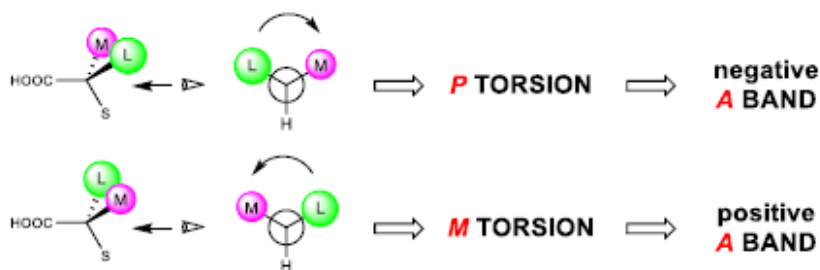

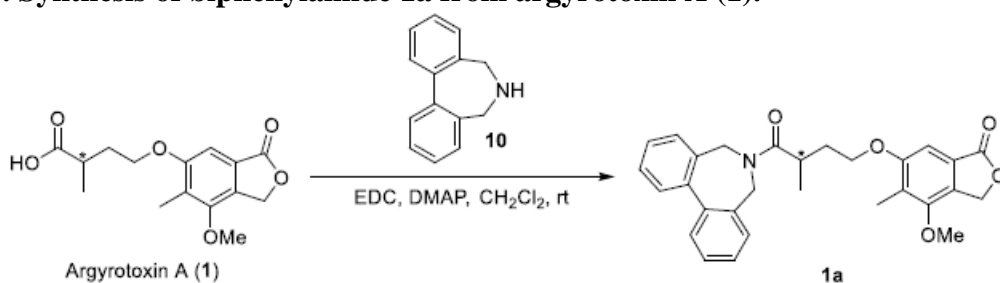**Fig. 4. Synthesis of biphenylamide 1a from argyrotoxin A (1).**

Fig. 5. UV and ECD spectra (CH₃CN) of biphenylamide 1a. Being the spectra recorded on crude mixture, values on vertical axes are on arbitrary units.